Science Press

ARTICLE

Plastic Deformation Behavior of 5A02 Aluminum Alloy Sheet at High Temperature

Jia Xiangdong[1,2], Yuan Rongjuan[2], He Liuyang[2], Cao Miaoyan[2], Wang Rui[3], Zhao Changcai[2]

[1] Nanjing Forestry University, Nanjing 210037, China; [2] Yanshan University, Qinhuangdao 066004, China; [3] Shandong University of Science and Technology, Qingdao 266590, China

Abstract: Taking 5A02 aluminum alloy cold-rolled sheet as the research object, the plastic deformation behavior of 5A02 aluminum alloy at different temperatures and strain rates was analyzed through uniaxial tensile test and metallographic test. Through combining experimental data and Zener-Hollomon parameter model, the constitutive model of 5A02 aluminum alloy under high temperature conditions was studied. The results show that the strain rate and deformation temperature have a great influence on the elongation when the 5A02 aluminum alloy is deformed under high temperature conditions. At strain rates of 0.01, 0.001, 0.0005 and 0.0001 s^{-1}, the elongation of 5A02 aluminum alloy is greater than 100% when the deformation temperature is above 250 °C. The true stress-strain curve of 5A02 aluminum alloy is characterized by dynamic recovery when the deformation temperature is 150~250 °C, and the flow stress curve has obvious softening phenomenon when the deformation temperature is above 250 °C.

Key words: aluminum alloy; high temperature deformation; plastic properties; flow stress; constitutive model

With the development of industrial technology and the rising of energy issues, lightweight design has become the primary design principle in the aerospace, automotive, rail transportation, electronics, communications and other industrial fields[1]. Therefore, the application and forming technology of lightweight alloy materials represented by aluminum alloys has become one of the focus and hot topics in current research[2-4].

Abedrabbo et al[5] studied the hardening model and anisotropic parameters of AA3003 aluminum alloy at different temperatures and strain rates, and then established an anisotropic material model of aluminum alloy that can be used for thermo-mechanical coupling finite element analysis. Soer et al[6] used the transmission electron microscope (TEM) to analyze the microstructure and dislocation substructure during the deformation in order to determine the superplastic deformation mechanism and the optimal de-

formation parameters of the aluminum-magnesium alloy, and then established a function relation between dislocation and strain, strain rate and temperature. Jia et al[7] studied the effect of Sc content on the nucleation and precipitation of the second phase by adding trace element Sc to Al-0.11% Zr alloy. The results showed that the precipitation of secondary phase is more uniform with the increase of Sc content, and the more precipitation of the secondary phase Al$_3$(Sc, Zr), the higher the recrystallization temperature of the Al-Sc-Zr alloy. Sun et al[8] studied the superplastic properties of Al-Mg-Sc-Zr alloys. The results showed that dynamic recrystallization occurs during the superplastic deformation of Al-Mg-Sc-Zr alloys, and the precipitated second phase particles can effectively inhibit the growth of coarse grains at the same time. Zhu et al[9] studied the thermal deformation behavior of 2050 Al-Li alloy under hot compression, and the flow stress curve was modified based

on the influence of friction and temperature difference on the flow stress. Gao et al [10] used scanning electron microscope (SEM), transmission electron microscope (TEM), tensile test and differential scanning calorimetry (DSC) to investigate the effects of different solution methods on microstructure, mechanical properties and precipitation behavior of Al-Mg-Si alloy. The results revealed that the recrystallized grains of the alloy after the solution treatment with hot air become smaller and more uniform, compared with solution treatment with electrical resistance. Chamanfar et al[11] established the constitutive model of AA6099 aluminum alloy using a power-law empirical model, and revealed the microstructures and dynamic softening mechanisms of the alloy under various deformation conditions by light optical microscopy (OM) and electron back scattered diffraction (EBSD) techniques. The results show that the main flow softening mechanism for AA6099 is dynamic recovery, and the partial dynamic recrystallization enhances the flow softening, especially at low deformation temperatures and high strain rates. Using the same research method, Li et al[12] studied the flow softening behavior and microstructure evolution of Al-5Zn-2Mg(7005) aluminum alloy during dynamic recovery, and results indicated that the remaining softening after deformation heating correction at high strain rate and the softening observed at high temperature are associated with grain coarsening induced by grain boundary migration during dynamic recovery process. He et al [13] studied the plastic deformation behavior of 2024 aluminum alloy at elevated temperatures by uniaxial hot tensile tests. In order to calculate the local stress-strain curves for different points of the specimen, the digital image correlation system was applied to determine the strain distribution during uniaxial tensile tests.

5××× is a kind of aluminum-magnesium alloy. With good forming performance and corrosion resistance, it is widely used in aviation, automotive and rail transportation [14,15]. In order to obtain the optimum deformation temperature and strain rate of 5083 aluminum alloy during superplastic forming, Hosseinipour[16] conducted a thermal uniaxial tensile test and scanning electron microscope for 5083 aluminum alloy sheet. The stress-strain relationship, strain rate sensitivity coefficient and pore volume fraction were determined at different temperatures and strain rates. Zhang et al[17] studied the superplastic deformation mechanism of annealed 5A90 aluminum alloy using uniaxial tensile test and scanning electron microscopy, and pointed out that the superplastic elongation of 5A90 aluminum alloy after recrystallization annealing can be significantly improved. Based on the M-K theory and numerical simulation techniques, Kapoor et al[18] studied the plastic forming properties of 5086 aluminum alloys at 20~200 °C and predicted the ultimate strain of 5086 aluminum alloys. Rudia et al[19] studied the isothermal hot deformation behavior of alumi-

num alloy 5083+15 wt% SiC composite through compression test, and established the constitutive equations based on modified Johnson-Cook model and modified Zerilli-Armstrong model to predict the hot flow behavior of the composite. Through the research, Rudia indicated that the hot flow stresses of 5083+15 wt% SiC depend on temperature and strain rate significantly, and both the models can give good description of the deformation behavior.

In the process of metal plastic forming, the construction of metal constitutive model is the basis of process simulation and process testing[20]. In order to investigate the flow behavior of 2219 aluminum alloys during warm deformation, Liu et al[21] conducted the thermal compression tests on 2219 aluminum alloy under various temperature and strain rate conditions with Gleeble-3500 thermomechanical simulation press, and determined the modification method of conventional Arrhenius-type constitutive model. On this basis, Liu et al established the constitutive equations of 2219 aluminum alloys under thermal compression deformation. Quan et al[22] determined the influence of deformation temperature and strain rate on the flow stress characteristics of 7075 aluminum alloy through the isothermal compressive tests, and established the constitutive model based on an artificial neural network (ANN) with back-propagation (BP) algorithm. The results indicated that the well-trained ANN model with BP algorithm has excellent capability to deal with the complex flow behaviors of as-extruded 7075 aluminum alloy and has great application potentiality in hot deformation process prediction. In order to characterize the flow behavior of 6083 aluminum alloy in hot compressive tests, Li et al[23] analyzed the experimental data by the phenomenological Arrhenius-type model, the physically based Estrin and Mecking (EM) model+Avrami equation, and an artificial neural network model; results indicated that the Arrhenius-type model is simpler and more efficient than the EM+Avrami model. Moreover, the well-trained ANN model has the best predicting performance. Liu et al[24] established the constitutive model of Al-Mg-Si-Mn-Cr alloy under thermal deformation conditions using the Johnson-Cook model, modified Zerilli-Armstrong model and strain-compensated Arrhenius model, and compared the results of the three prediction models with the experimental data. The results showed that the three models are able to predict the flow behavior of the alloy. Strain-compensated Arrhenius model has the best simulation ability in predicting flow stresses, while the modified Johnson-Cook model has lower prediction accuracy and the modified Zerilli-Armstrong model has poorer predictive ability at low strain rates. It can be seen from the above research that the recovery and recrystallization will occur in aluminum alloy sheet during thermal deformation, and the true stress-strain curve is obviously softened, and these characteristics should be considered in the construction of alumi-

num alloy constitutive model. The most widely used constitutive model includes Johnson-Cook model, Zerilli-Armstrong model, Arrhenius-type model, etc.

In this study, the 5A02 aluminum alloy cold-rolled sheet was used as the study object. The deformation characteristics of 5A02 aluminum alloy sheet under the conditions of different temperatures and strain rates were studied by uniaxial tensile test and metallographic analysis.

1 Experiment

1.1 Uniaxial tensile test

In order to obtain the plastic performance index of aluminum alloy at high temperature, the 5A02 aluminum alloy cold-rolled sheet was selected as the base material during the study. The composition of the selected test sheet was obtained by spectral analyzer, as shown in Table 1.

Along the rolling direction of the test sheet, uniaxial tensile specimens were obtained by wire cutting equipment. The sample size is shown in Fig.1. The uniaxial tensile test was performed on the INSPEKT Table 100 kN electronic universal material testing machine (Fig.2) according to the parameters shown in Table 2. The tensile specimen was heated by the electronic universal material testing machine according to the test setting parameters. The sample was completely placed in the heating furnace during the entire uniaxial tensile test, which provides a constant temperature environment.

Table 1   Composition of 5A02 cold rolled sheet used in the test (wt%)

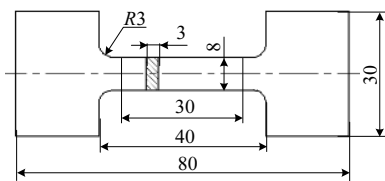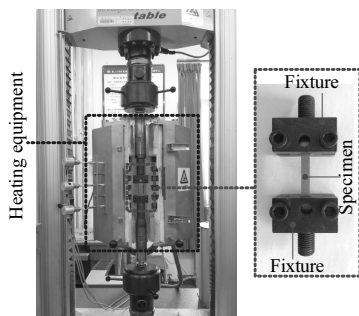| Si	Fe	Cu	Mg	Cr	Ti	Al
0.10	0.20	0.05	2.60	0.25	0.05	Bal.

Fig.1   Specimen for uniaxial tensile test

Fig.2   Equipment of uniaxial tensile test

1.2 Metallographic analysis

The 5A02 aluminum alloy used in this study belongs to Al-Mg series aluminum alloys, and the thermal deformation process is affected by heating temperature, holding time, deformation rate, deformation degree and other factors. When the 5A02 aluminum alloy sheet is deformed in the high temperature environment, it will undergo recovery and recrystallization and the change of the metallographic structure will lead to the change of plastic properties. In order to clarify the reasons for the change of plastic properties of 5A02 aluminum alloy sheet at high temperature, metallographic specimens were prepared by electrolytic polishing and anodizing.

2 Results and Discussion

2.1 Specific elongation

The curve of the elongation of 5A02 aluminum alloy at high temperature with the change of temperature obtained by the uniaxial tensile test is shown in Fig.3. From the test results, it can be seen that under the same strain rate conditions, the elongation gradually increases as the temperature increases when the deformation temperature is between 150 °C and 350 °C. At strain rates of 0.01 and 0.001 s^{-1}, the elongation to fracture of the specimen shows an overall increase trend when the deformation temperature increases from 350 °C to 450 °C, and reaches the maximum at 400~425 °C. At the strain rates of 0.0001 and 0.0005 s^{-1}, the elongation of the specimens tends to decrease when the deformation temperature increases from 350 °C to 450 °C.

From the elongation curves shown in Fig.3, it can be seen that the elongation of 5A02 is greater than 100% when the tensile temperature is greater than 250 °C.

Comparing the temperature at the maximum elongation under different strain rate conditions shown in Fig.3a and Fig.3b, it can be seen that the temperature at which the maximum elongation is reached is significantly lower under the conditions of lower strain rate (0.0001 and 0.0005 s^{-1}) compared to under the conditions of higher strain rate (0.01 and 0.001 s^{-1}).

Table 2   Parameters setting of tensile test

Temperature/ °C	Heating rate/ °C·min^{-1}	Holding time/ min	Strain rate/ s^{-1}
150	10	15	
200	10	15	
250	10	15	0.01
300	20	15	0.001
350	20	15	0.0005
400	20	15	0.0001
425	20	15	
450	20	15	

From the relationship curves of strain rate and elongation shown in Fig.4a, it can be seen that the elongation to fracture of the specimen gradually increases as the strain rate decreases when the deformation temperature is lower than 350 °C. However, the pattern shown in Fig.4a will no longer exist when the deformation temperature continues to rise above 400 °C, especially at the deformation temperature of 425 and 450 °C. As the strain rate decreases, the elongation of the specimen also decreases, as shown in Fig.4b.

2.2 Metallographic analysis

The original sheet metal was rapidly cooled after holding at 350, 400 and 450 °C for 60 min. The corresponding microstructures of the sheet metal are obtained, as shown in Fig.5.

The 5A02 aluminum alloy used in this study is annealed, and the fibrous structure of the sheet metal in the rolling plane disappears, as shown in Fig.5a. The comparison of the metallographic results between the original sheet and the sheet after heat treatment shows that the recrystallization of 5A02 aluminum alloy occurs in different degrees during the heating process. By comparing the grain sizes at different temperatures, the grain morphology of the sheet
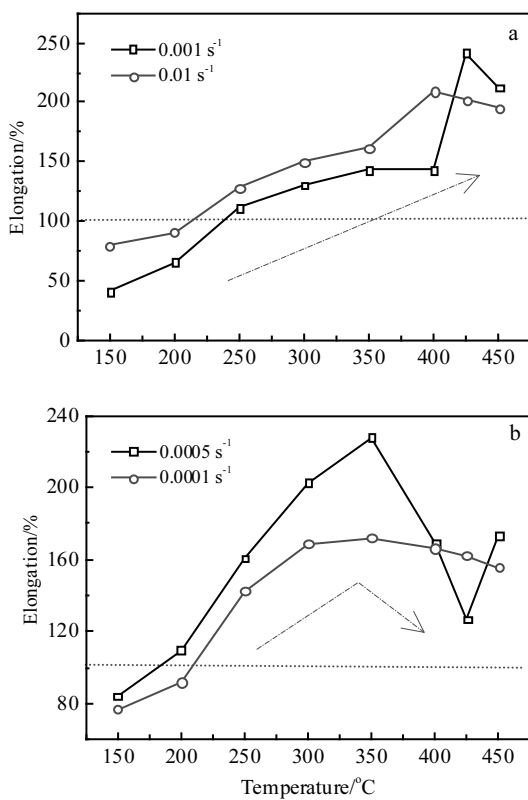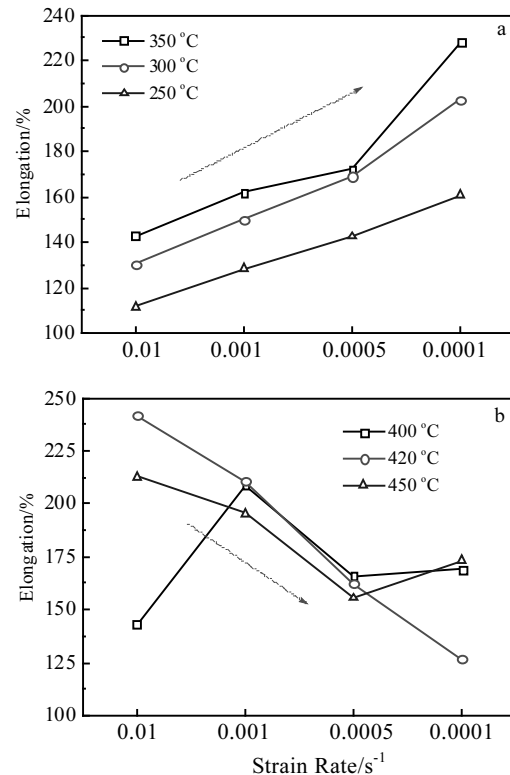

Fig.4   Elongation curves at relatively lower (a) and higher (b) temperatures

shows little difference between the sheet metal and the parent metal at 350 °C, except some new small grains are generated between individual grains. The irregularly shaped grains in the original base metal disappear, and the grain size of the sheet metal tends to be uniform at 400 °C. The grains grow significantly when the temperature is increased to 450 °C. Therefore, the grain sizes of 5A02 aluminum alloy under high temperature conditions can be greatly affected by temperature and holding time. The higher the temperature and the longer the holding time, the greater the grain size of sheet metal can be obtained.

In order the further analyze the cause of the change of elongation rate in the uniaxial tensile test, the metallurgical structures of the aluminum alloy sheet after the tensile deformation at 400 and 450 °C were studied. The obtained metallographic structure is shown in Fig.6 and Fig.7.

The grain of the 5A02 aluminum alloy sheet is significantly elongated along the deformation direction after deformation under the effect of higher strain rate (0.01, 0.001 s^{-1}), as shown in Fig.6 and Fig.7. This indicates that the deformation is mainly concentrated inside the grains under high temperature and high strain rate conditions, which is mainly caused by dislocation slip in the crystal. Under

Fig.3   Elongation curves at relatively higher (a) and lower (b) strain rates
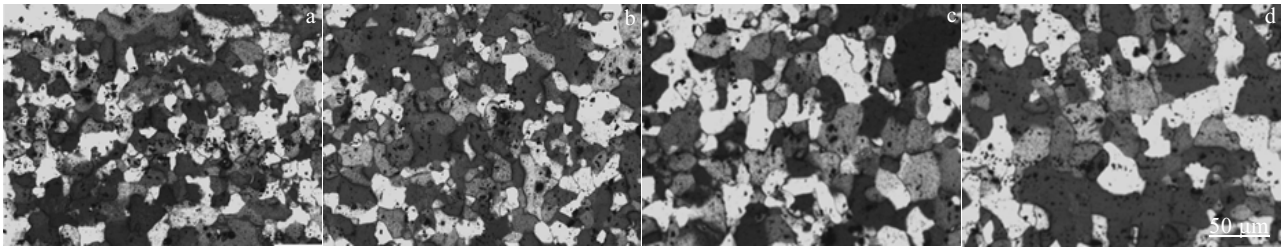
Fig.5   Microstructures of 5A02 aluminum alloy preserved at different temperatures: (a) initial state, (b) 350 °C, (c) 400 °C, and (d) 450 °C
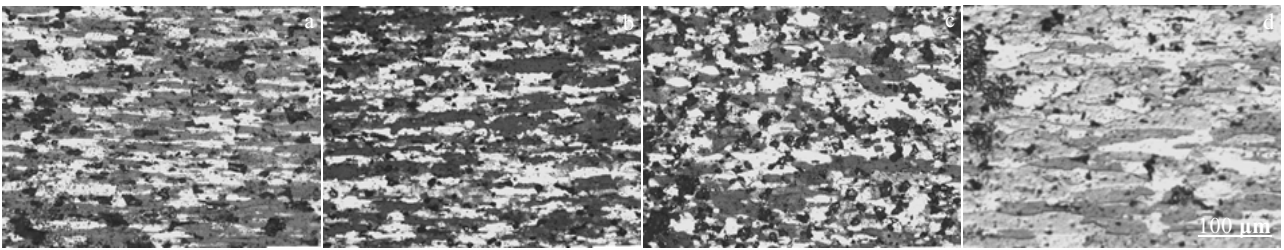

Fig.6   Metallographic structure after tensile deformation at 400 °C at different strain rates: (a) 0.01 s^{-1}, (b) 0.001 s^{-1}, (c) 0.0005 s^{-1}, and (d) 0.0001 s^{-1}
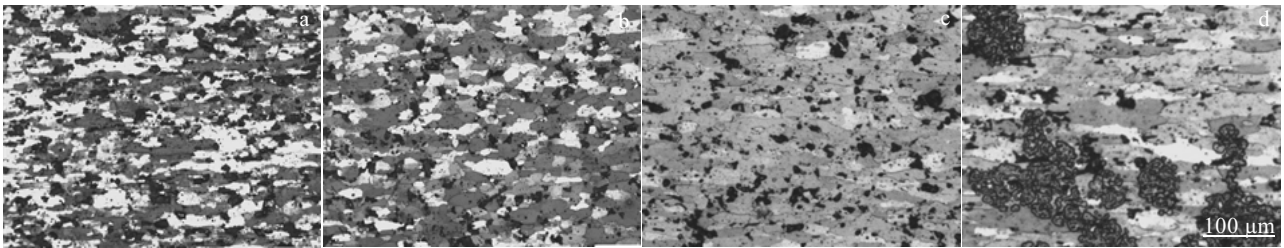

Fig.7   Metallographic structures after tensile deformation at 450 °C at different strain rates: (a) 0.01 s^{-1}, (b) 0.001 s^{-1}, (c) 0.0005 s^{-1}, and (d) 0.0001 s^{-1}

low strain rate conditions (0.0005, 0.0001 s^{-1}), the grain is elongated along the deformation direction with obvious grain growth. There is obvious precipitation of the second phase near the grain boundary, which will make it difficult to carry out the slip of grain boundary and grain rotation, thus leading to stress concentration in the area near the grain boundary. Therefore, the plastic deformation performance of 5A02 aluminum alloy is reduced. Comparing the results of Fig.6 and Fig.7, the tendency of the grain growth of the sheet is more obvious as the deformation temperature increases and the deformation rate decreases during the deformation process.

It can be concluded that the strain rate and deformation temperature have a great influence on the elongation of 5A02 aluminum alloy when it is deformed under high temperature condition by combining metallographic test results and elongation test results. The elongation increases with the decrease of strain rate when the deformation temperature is less than 350 °C. This is because the time is consumed by the softening mechanism such as grain boundary

diffusion, dynamic recovery and dynamic recrystallization of 5A02 aluminum alloy plastic deformation, and the deformation time increases with the decrease of strain rate; the aluminum alloy has enough time to soften to counteract the stress concentration caused by the work hardening, thus increasing the elongation of 5A02 aluminum alloy. However, the elongation rate decreases with the decrease of strain rate when the deformation temperature is greater than 400 °C. This is because the holding time of the 5A02 aluminum alloy under high temperature environment is increased with the decrease of strain rate, and the grains are easy to grow up and to coarsen, and the impurity elements and the second phase precipitate along the grain boundaries, which makes it difficult to carry out grain boundary slip and grain rotation, thus leading to the reduction of elongation.

2.3   True stress-strain curves

Fig.8 shows the true stress-strain curves of 5A02 aluminum alloy at 150~300 °C. It can be seen from Fig.8 that true stress increases with true strain at 150 and 200 °C. At the deformation temperature of 250 and 300 °C at a certain

strain rate, the true strain has little effect on the true stress when the true strain exceeds a certain value, manifesting a distinct steady-state rheological characteristic, and the steady state flow stress decreases as the deformation temperature increases.

Fig.9 shows the true stress-strain curves of 5A02 aluminum alloy at 350~450 °C. It can be clearly seen that there is an obvious softening phenomenon in the deformation of 5A02 aluminum alloy under this temperature condition. The higher the deformation temperature and the slower the strain rate, the more obvious the deformation softening phenomenon.

Comparing the true stress-strain curves in Fig.8 and Fig.9, the true stress of 5A02 aluminum alloy decreases as the strain rate decreases under the same temperature condition. With the same strain rate, the true stress gradually decreases as the deformation temperature increases. Under the same temperature and strain rate condition, the true stress of 5A02 aluminum alloy increases rapidly with the increase of true strain first, but the slope of the true stress-strain curve gradually decreases with the increase of cumulative strain.

Combining the obtained true stress-strain curves of 5A02 aluminum alloy with the elongation and metallographic structure, it can be concluded that the heating temperature, holding time and deformation rate have a great influence on the plastic properties of 5A02 aluminum alloy under high temperature condition. 5A02 aluminum alloy belongs to the materials that are sensitive to the deformation temperature and the deformation rate.

3 Constitutive Model

According to the true stress-strain curve of the 5A02 aluminum alloy obtained from the experiment, the true stress-strain curve of the 5A02 aluminum alloy belongs to the dynamic recovery type at deformation temperatures of 150 and 200 °C and it can be fitted with the common exponential function constitutive model. When the deformation temperature is greater than 250 °C, the 5A02 aluminum alloy exhibits superplasticity. The true stress does not increase with the increase of true strain, and the true stress is greatly affected by the strain rate and deformation temperature. Therefore, the following research will focus on the constitutive model of 5A02 aluminum alloy at deformation temperatures greater than 250 °C.

Existing research results have shown that the deformation of aluminum alloy under high temperature conditions is affected by the activation energy[25], and true stress-strain curve can be expressed by Eq.(1).

$$\sigma = f(\varepsilon, z) \tag{1}$$

where σ is the peak stress or steady-state flow stress, ε is the true strain and Z is the Zener-Hollomon parameter which represents the relationship between strain rate $\dot{\varepsilon}$, deformation activation energy Q and deformation temperature T during the deformation process. Z can be obtained according to Eq.(2).

$$Z = \dot{\varepsilon}\exp\left[Q/(RT)\right] \tag{2}$$

where R is the molar gas constant, R=8.31 J/K·mol.

Under the condition of low strain, the flow stress σ and strain rate $\dot{\varepsilon}$ have an exponential relationship, as shown in
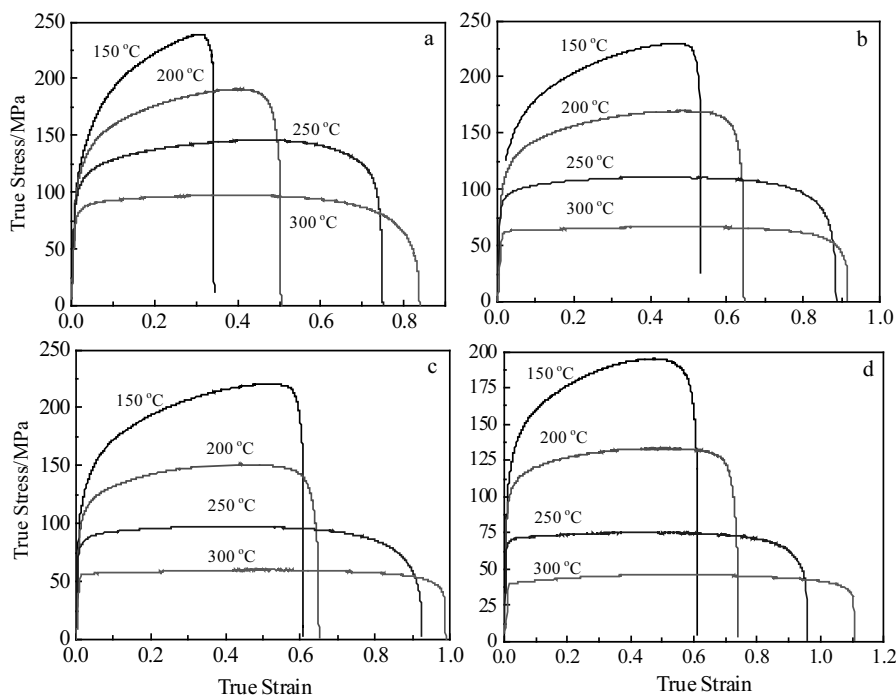

Fig.8   Stress-strain curves of 5A02 aluminum alloy at temperatures below 300 °C at different strain rates: (a) 0.01 s⁻¹, (b) 0.001 s⁻¹, (c) 0.0005 s⁻¹, and (d) 0.0001 s⁻¹
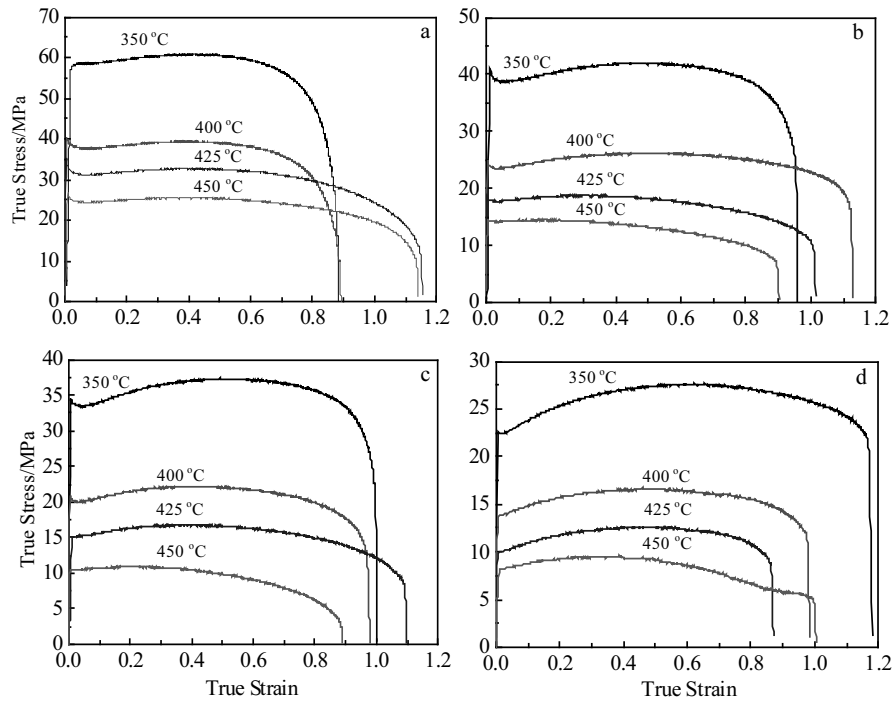
Fig.9　Stress-strain curves of 5A02 aluminum alloy at temperatures above 350 °C at different strain rates: (a) 0.01 s⁻¹, (b) 0.001 s⁻¹, (c) 0.0005 s⁻¹, and (d) 0.0001 s⁻¹

Eq.(3). Under the condition of high stress, the relationship between flow stress σ and strain rate $\dot{\varepsilon}$ satisfies the function of Eq.(4).

$$\dot{\varepsilon}=A_1\sigma^{n'},\ \alpha\sigma < 0.8 \tag{3}$$

$$\dot{\varepsilon}=A_2\exp(\beta\sigma),\ \alpha\sigma > 1.2 \tag{4}$$

where A_1, A_2, α, β and n' are temperature independent material constants, and α, β, and n' satisfy the relationship of $\alpha=\beta/n'$.

Senars and Tegart established the Arrhenius relationship of the flow stress, strain rate, and temperature at any stress level[24,25], which is modified by the hyperbolic sine form containing the deformation activation energy and the deformation temperature when the material is deformed in a high temperature environment.

$$\dot{\varepsilon}=A\left[\sinh\left(\alpha\sigma\right)\right]^{n}\exp\left[-Q/\left(RT\right)\right] \tag{5}$$

where A and n are temperature independent material constants.

Substituting Eq.(5) into Eq.(2), parameter Z of Zener-Hollomon model can be expressed as follows:

$$Z=A\left[\sinh(\alpha\sigma)\right]^{n} \tag{6}$$

According to the definition of the hyperbolic sine func-

tion, the expression of the flow stress σ including the Z parameter can be obtained from Eq.(6).

$$\sigma=\frac{1}{\alpha}\ln\left\{\left(\frac{Z}{A}\right)^{1/n}+\left[\left(\frac{Z}{A}\right)^{2/n}+1\right]^{1/2}\right\} \tag{7}$$

Both sides of Eq.(3) and Eq.(4) are simultaneously logarithmic and sorted:

$$\ln\sigma=\frac{\ln\dot{\varepsilon}}{n'}-\frac{\ln A_1}{n'} \tag{8}$$

$$\sigma=\frac{\ln\dot{\varepsilon}}{\beta}-\frac{\ln A_2}{\beta} \tag{9}$$

It can be seen from Eq.(8) and Eq.(9) that when the temperature is constant, n' is the reciprocal of the slope of function $\ln\sigma$-$\ln\dot{\varepsilon}$, and β is the reciprocal of the slope of function σ-$\ln\dot{\varepsilon}$. The obtained experimental data can be analyzed by a linear regression analysis according to Eq.(8) and Eq.(9), and the relationship curves of $\ln\sigma$-$\ln\dot{\varepsilon}$ and σ-$\ln\dot{\varepsilon}$ can be obtained, as shown in Fig.10.

According to the results shown in Fig.10, n' and β under different temperature conditions are calculated, as shown in Table 3. The α value under different temperature conditions can be obtained by taking the n' and β into formula $\alpha=\beta/n'$.

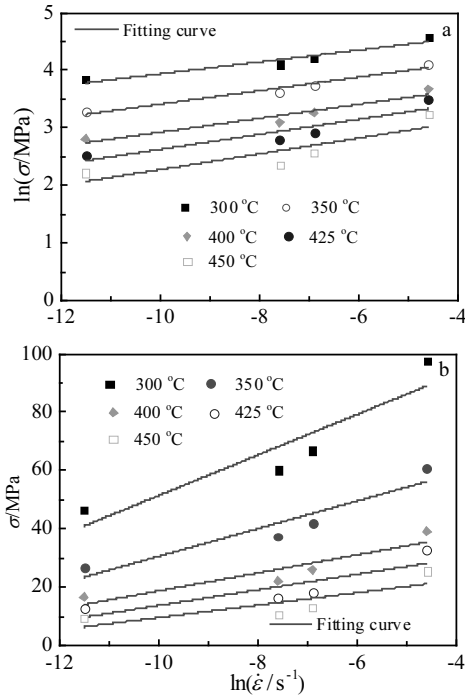Both sides of Eq.(5) are simultaneously logarithmic and sorted:

various temperature conditions shown in Table 3 with the data obtained from the experiment, the ln[sinh($\alpha\sigma$)]-ln $\dot{\varepsilon}$ curves and the ln[sinh($\alpha\sigma$)]-1/T curves are plotted using linear regression, as shown in Fig.11 and Fig.12. According to Fig.11 and Fig.12, n and A values under different temperature conditions are calculated, as shown in Table 4. The deformation activation energy Q under different strain rate conditions is obtained, as shown in Table 5.

Taking the calculated A, n, α, Q and other material parameters into Eq.(5~7), the constitutive model of 5A02 aluminum alloy under high temperature conditions can be obtained.

$$\dot{\varepsilon}=5.7 \times 10^{19} \left[\sinh \left(0.038\sigma \right) \right]^{5.43} \exp \left[-297.7 \big/ \left(RT \right) \right] \quad (13)$$

$$Z=5.7 \times 10^{19} \left[\sinh \left(0.038\sigma \right) \right]^{5.43} \quad (14)$$
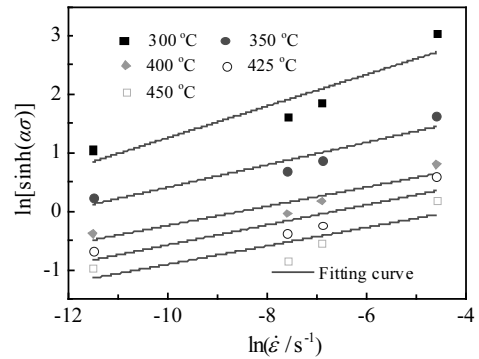

Fig.11   Regression analysis curves of ln[sinh($\alpha\sigma$)]-ln $\dot{\varepsilon}$

Fig.12   Regression analysis curves of ln[sinh($\alpha\sigma$)]-1/T

Fig.10   Regression analysis curves between flow stress and strain rate: (a) lnσ-ln $\dot{\varepsilon}$ and (b) σ-ln $\dot{\varepsilon}$

Table 3   Values of n', β and α at different temperatures

Parameter	Temperature/ °C					Average
	300	350	400	425	450	
n'	9.671	8.511	8.258	7.651	7.315	8.281
β/MPa^{-1}	0.144	0.211	0.323	0.374	0.496	0.304
α/MPa^{-1}	0.015	0.025	0.039	0.049	0.064	0.038

$$\ln \left[\sinh \left(\alpha\sigma \right) \right] = \frac{\ln\dot{\varepsilon}}{n} - \frac{\ln A}{n} + \frac{Q}{nRT} \quad (10)$$

When the deformation temperature is constant, the partial derivative of Eq.(10) for ln$\dot{\varepsilon}$ can be obtained.

$$\frac{1}{n} = \frac{\partial \left[\sinh \left(\alpha\sigma \right) \right]}{\partial \ln\dot{\varepsilon}} \quad (11)$$

When the strain rate is constant, the partial derivative of Eq.(10) for 1/T can be obtained.

$$Q=nR \frac{\partial \left[\sinh \left(\alpha\sigma \right) \right]}{\partial \left(1/T \right)} \quad (12)$$

It can be seen from Eq.(10) and Eq.(11) that the strain rate sensitivity index 1/n is the slope of linear function curve of ln[sinh($\alpha\sigma$)] with respect to ln$\dot{\varepsilon}$, and the intercept with the ordinate axis is Q/nRT−lnA/n. From Eq.(10) and Eq.(12), Q/nR is the slope of curve of the linear function ln[sinh($\alpha\sigma$)]-1/T.

Based on the analysis above, combining α values under

Table 4   Values of n and A at different temperatures

T/°C	300	350	400	425	450	Average
n	3.69	5.20	6.09	5.83	6.34	5.43
A/×10^{19}	0.16	1.9	7.2	5.0	14	5.7

Table 5   Values of Q at different strain rates

$\dot{\varepsilon}$ /s^{-1}	0.01	0.001	0.0005	0.0001	Average
Q/kJ·mol^{-1}	347.3	297.1	295.7	250.7	297.7

$$\sigma = \frac{1}{0.038} \ln \left\{ \left(\frac{Z}{5.7 \times 10^{19}} \right)^{1/5.43} + \left[\left(\frac{Z}{5.7 \times 10^{19}} \right)^{2/5.43} + 1 \right]^{1/2} \right\} \quad (15)$$

4 Conclusions

1) At the strain rates of 0.01, 0.001, 0.0005 and 0.0001 s^{-1}, the uniform elongation of the 5A02 aluminum alloy is greater than 100% when the deformation temperature is greater than 250 °C.

2) When 5A02 aluminum alloy is deformed under high temperature conditions, strain rate and deformation temperature have a great influence on the elongation of the material. The higher the heating temperature and the longer the holding time, the lower the uniform elongation of 5A02 aluminum alloy.

3) The true stress-strain curve of 5A02 aluminum alloy belongs to a dynamic recovery type when it is deformed at a lower temperature (150~250 °C). However, there is a significant softening phenomenon during deformation under high temperature conditions (>250 °C). The higher the deformation temperature and the slower the strain rate, the more obvious the deformation softening phenomenon.

References

1 Bressan J D, Bruschi S, Ghiotti A. *International Journal of Mechanical Sciences*[J], 2016, 115: 702

2 Wang N, Ilinich A, Chen M H *et al*. *International Journal of Mechanical Sciences*[J], 2019, 151: 444

3 Chen G, Lu L P, Ren C Z. *Journal of Alloys and Compounds*[J], 2018, 765: 569

4 Jiang D, Xu Y, Zhu D H *et al*. *Advances in Mechanical Engineering*[J], 2019, 11: 1

5 Abedrabbo N, Pourboghrat F, Carsley J. *International Journal of Plasticity*[J], 2006, 22: 342

6 Soer W A, Chezan A R, Hosson J T M D. *Acta Materialia*[J], 2006, 54: 3827

7 Jia Z H, Røyset J, Solberg J K *et al*. *Transactions of Nonferrous Metals Society of China*[J], 2012, 22: 1866

8 Sun X, Pan Q L, Li M J *et al*. *The Chinese Journal of Nonferrous Metals*[J], 2016, 26: 280 (in Chinese)

9 Zhu R H, Liu Q, Li J F *et al*. *Transactions of Nonferrous Metals Society of China*[J], 2018, 28(3): 404

10 Gao G J, He C, Li Y *et al*. *Transactions of Nonferrous Metals Society of China*[J], 2018, 28(5): 839

11 Chamanfar A, Alamoudi M T, Nanninga N E. *Materials Science and Engineering A*[J], 2019, 743: 684

12 Li L X, Wang G, Liu J *et al*. *Transactions of Nonferrous Metals Society of China*[J], 2014, 24: 42

13 He Z B, Wang Z B, Lin Y L *et al*. *Metals*[J], 2019, 9: 243

14 Howeyze M, Eivani A R, Arabi H *et al*. *Materials Science and Engineering A*[J], 2018, 732: 120

15 Zayed E M, El-Tayeb N S M, Ahmed M M Z *et al*. *Engineering Design Applications*[J], 2019, 92: 11

16 Hosseinipour S J. *Advanced Materials Research*[J], 2009, 83-86: 400

17 Zhang P, Ye L Y, Gu G *et al*. *Journal of Materials Engineering*[J], 2014, 9: 51

18 Kapoor I, Narayanan R G, Taylor S *et al*. *Procedia Engineering*[J], 2017, 173: 897

19 Rudra A, Das S, Dasgupta R. *Journal of Materials Engineering and Performance*[J], 2019, 28: 87

20 Liu B S, Lang L H, Li H L *et al*. *Journal of Plasticity Engineering*[J], 2011, 18: 53 (in Chinese)

21 Liu L, Wu Y X, Gong H *et al*. *Transactions of Nonferrous Metals Society of China*[J], 2019, 29: 448

22 Quan G Z, Zou Z Y, Wang T *et al*. *High Temperature Materials and Processes*[J], 2017, 36: 1

23 Li K, Pan Q l, Li R S. *Journal of Materials Engineering and Performance*[J], 2019, 28: 981

24 Liu S H, Pan Q L, Li H *et al*. *Journal of Materials Science*[J], 2019, 54: 4366

25 Wang Y, Pan Q L, Song Y F *et al*. *Transactions of Nonferrous Metals Society of China*[J], 2013, 23(11): 3235

高温变形条件下 5A02 铝合金的塑性成形性能

贾向东[1,2]，袁荣娟[2]，何留洋[2]，曹秒艳[2]，王 瑞[3]，赵长财[2]
(1. 南京林业大学，江苏 南京 210037)
(2. 燕山大学，河北 秦皇岛 066004)
(3. 山东科技大学，山东 青岛 266590)

摘 要：以 5A02 铝合金冷轧板材为研究对象，通过单向拉伸试验和金相试验对不同变形温度、应变速率条件下 5A02 铝合金的塑性能进行分析，并且借助试验数据和 Zener-Hollomon 参数模型，对高温条件下 5A02 铝合金的本构模型进行研究。结果表明：5A02 铝合金在高温条件下变形时，应变速率和变形温度对延伸率的影响很大。在应变速率为 0.01、0.001、0.0005 和 0.0001 s^{-1} 条件下，当变形温度大于 250 ℃时，5A02 铝合金的延伸率大于 100%。当变形温度为 150~250 ℃时，5A02 铝合金的真实应力-应变曲线属于动态回复型，而当变形温度大于 250 ℃时，流变应力曲线存在明显的软化现象。
关键词：5A02铝合金；高温拉伸；塑性性能；流变应力；本构模型

作者简介：贾向东，男，1987 年生，博士，讲师，南京林业大学机械电子工程学院，江苏 南京 210037，E-mail: jiaxd.good@njfu.edu.cn